PAPR Reduction for STBC Transmit Diversity with Transmit FDE using Blind Selected Mapping

Amnart Boonkajay* and Fumiyuki Adachi†
Research Organization of Electrical Communication (ROEC), Tohoku University
2-1-1 Katahira, Aoba-ku, Sendai, Miyagi, 980-8577 Japan
E-mail: *amnart@riec.tohoku.ac.jp, †adachi@ecei.tohoku.ac.jp

***Abstract*—Recently, we have proposed a peak-to-average power ratio (PAPR) reduction technique called blind selected mapping (blind SLM) for single-antenna transmission and for space-time block coded transmit diversity (STBC-TD). Blind SLM does not require side-information transmission. We exploited the fact that PAPR of the signal after STBC encoding and that of before STBC encoding are the same. However, if STBC-TD is combined with transmit frequency-domain equalization (Tx-FDE), this does not hold anymore. In this paper, we study an application of blind SLM on STBC-TD with Tx-FDE. Both orthogonal frequency division multiplexing (OFDM) and discrete Fourier transform (DFT)-precoded OFDM transmissions are considered. Phase rotation sequence selection in SLM is carried out to minimize the maximum instantaneous PAPR among all transmit antennas. Computer simulation results confirm that blind SLM can reduce the PAPR of STBC-TD with Tx-FDE without causing significant bit-error rate (BER) degradation when the total received bit energy-per-noise power spectrum density (E_b/N_0) is higher than about 5 dB.**

***Index Terms*—OFDM, DFT-precoded OFDM, SLM, PAPR, STBC**

I. Introduction

High-frequency bands, e.g. centimeter and millimeter waves, are expected to be used in the next-generation mobile communication networks due to its abundant bandwidth availability [1]. Therefore, peak-to-average power ratio (PAPR) reduction is still an important issue since the high power amplifier (HPA) suffers from low amplification efficiency when operating at high carrier frequency [2]. PAPR properties of orthogonal frequency division multiplexing (OFDM) and single-carrier (SC) have been well studied [3]. OFDM waveform generally has higher PAPR than SC waveform, but the PAPR of SC is sensitive to high-level data modulation and transmit filtering, especially when the SC signal is generated by mean of discrete Fourier transform (DFT)-precoded OFDM [4].

Among various PAPR reduction techniques, selected mapping (SLM) [5] is well-known as an efficient, simple PAPR reduction technique. SLM generates multiple transmit waveform candidates by multiplying the original signal waveform with various phase rotation sequences and then selecting the waveform with the lowest PAPR. The proposed SLM in [5] is originally for OFDM and requires side-information (e.g. the selected phase rotation sequence number) transmission. We recently proposed the blind SLM for filtered SC [6], where the phase rotation is conducted in time domain. Maximum likelihood (ML) phase sequence estimation or 2-step estimation based on Viterbi algorithm [7] can be employed at the receiver and hence no side-information transmission is required.

Space-time block-coded transmit diversity (STBC-TD) [8] is a powerful technique to improve the transmission quality in a fading environment. Blind SLM for STBC-TD [9] was studied by exploiting a fact that the PAPR of signals before STBC encoding and after STBC encoding are the same. STBC-TD is typically equipped with receive frequency-domain equalization (Rx-FDE) and is able to support arbitrary number of receive antennas, but transmission rate is reduced if the number of transmit antennas increases. On the other hand, STBC-TD equipped with transmit FDE (Tx-FDE) [10] can support an arbitrary number of transmit antennas. However, the PAPRs of signals before encoding and after encoding become different because of addition/subtraction operation and multiplication of FDE weights (note that only complex conjugate operation is involved in the case of STBC-TD without Tx-FDE).

In this paper, we focus on the PAPR problem of STBC-TD with Tx-FDE and study an application of blind SLM to STBC-TD with Tx-FDE. Both OFDM and SC signals are considered. In the SLM stage, phase rotation is applied prior to STBC encoding and Tx-FDE in order to preserve the STBC code orthogonality. Phase rotation sequence is selected in order to minimize the maximum instantaneous PAPR among all transmit antennas (hereinafter called the minimax criterion). PAPR and bit-error rate (BER) of STBC-TD with Tx-FDE and blind SLM is evaluated by computer simulation to confirm that the PAPR can be reduced with no significant BER degradation when the received signal power is sufficiently high. Moreover, we found from the simulation results that the PAPRs of OFDM and SC signals are not different when STBC-TD with Tx-FDE and blind SLM are used.

II. STBC-TD transmitter with Tx-FDE and SLM

STBC-TD transmitter with Tx-FDE and blind SLM is illustrated by Fig. 1. The transmitter is equipped with N_t transmit antennas, and the receiver is equipped with N_r receive antennas (the receiver will be described in details in Sect.III).

A. Transmit signal representation

We begin with J blocks of N_c-length data-modulated transmit symbols $\{d_j(n); n = 0 \sim N_c - 1, j = 0 \sim J - 1\}$. Phase rotation is multiplied to the data-modulated blocks. A common phase rotation sequence $\{p_{\hat{m}}(n); n = 0 \sim N_c - 1\}$ is selected by SLM algorithm where $\hat{m} \in 0 \sim M - 1$ and

M is the number of available phase rotation sequences in a predefined codebook. We assume $\hat{m}$ to be the same for all J blocks. The selection of $\{p_{\hat{m}}(n)\}$ will be described in Sect.II-B. J blocks of N_c-length phase-rotated symbols $\{d_{j,\hat{m}}(n); n = 0 \sim N_c - 1, j = 0 \sim J - 1\}$ is defined as

$$d_{j,\hat{m}}(n) = p_{\hat{m}}(n) d_j(n). \tag{1}$$

In the case of SC transmission, $\{d_{j,\hat{m}}(n)\}$ is then transformed into frequency domain by N_c-point DFT, yielding J blocks of frequency components $\{D_{j,\hat{m}}(k); k = 0 \sim N_c - 1, j = 0 \sim J - 1\}$. The frequency components blocks before STBC encoding $\{D_{j,\hat{m}}(k)\}$ is expressed by

$$D_{j,\hat{m}}(k) = \begin{cases} \frac{1}{\sqrt{N_c}} \sum\limits_{n=0}^{N_c-1} d_{j,\hat{m}}(n) \exp(-i2\pi \frac{kn}{N_c}) & \text{for SC,} \\ d_{j,\hat{m}}(k) & \text{for OFDM,} \end{cases} \tag{2}$$

where $i = \sqrt{-1}$. Next, J blocks of $\{D_{j,\hat{m}}(k)\}$ are STBC encoded, yielding N_t parallel streams of Q encoded frequency component blocks. The STBC encoding process for each frequency index k can be represented by an $N_r \times Q$ matrix $\mathbf{X}_{\hat{m}}(k)$ [8]. $\mathbf{X}_{\hat{m}}(k)$ depends on N_r and is expressed in [10]. In this paper, we assume N_r=2 for simplicity. N_t can be arbitrary. $\mathbf{X}_{\hat{m}}(k)$ is expressed by

$$\mathbf{X}_{\hat{m}}(k) = \begin{cases} D_{0,\hat{m}}(k) & \text{if } N_t = 1, \\ \begin{bmatrix} D_{0,\hat{m}}(k) & -D^*_{1,\hat{m}}(k) \\ D_{1,\hat{m}}(k) & D^*_{0,\hat{m}}(k) \end{bmatrix} & \text{if } N_t = 2. \end{cases} \tag{3}$$

In addition, the STBC encoding parameters N_r, J and Q, and the corresponding coding rate R_{STBC}=J/Q, are shown in [10]. If N_r=2, J=Q=2 and R_{STBC}=1, meaning that the transmission rate can be kept the same as single-antenna case.

Tx-FDE is applied after STBC encoding, where the Tx-FDE weight matrix at the k-th subcarrier can be represented by an $N_t \times N_r$ matrix $\mathbf{W}_t(k)$. The frequency-domain transmit signal matrix at the k-th subcarrier, $\mathbf{S}_{\hat{m}}(k)$, with the dimension of $N_t \times Q$ is given by

$$\mathbf{S}_{\hat{m}}(k) = A\mathbf{W}_t(k)\mathbf{X}_{\hat{m}}(k), \tag{4}$$

where A represents the power normalization factor. In this paper, we use the minimum mean-square error based FDE (MMSE-FDE) for both OFDM and SC transmissions. The FDE weight at the n_t-th row and the n_r-th column, $\mathbf{W}_t(k; n_t, n_r)$, is expressed by [10]

$$\mathbf{W}_t(k; n_t, n_r) = \frac{H^*(k; n_r, n_t)}{\frac{1}{N_r} \sum\limits_{n_r=0}^{N_r-1} |H(k; n_r, n_t)|^2 + (E_s/N_0)^{-1}}, \tag{5}$$

where $H(k; n_r, n_t)$ is an element at the n_r-th row and the n_t-th column of multi-input multi-output (MIMO) channel transfer function at the k-th subcarrier, $\mathbf{H}(k), k = 0 \sim N_c - 1$. E_s represents symbol energy and N_0 is one-sided noise power spectrum density.

After applying Tx-FDE, the q-th frequency-domain block at the n_t-th transmit antenna $\{S_{\hat{m}}(k; n_t, q); k = 0 \sim N_c - 1\}$

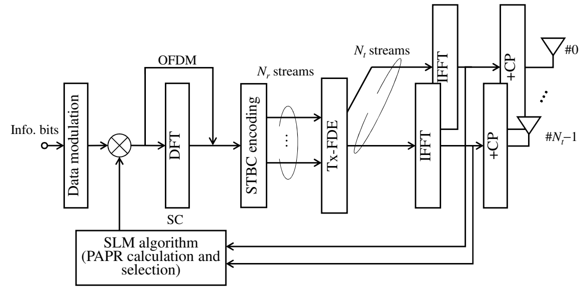

Fig. 1. Transmitter of STBC-TD with Tx-FDE and blind SLM.

is transformed to time-domain signal $\{s_{\hat{m}}(n; n_t, q); n = 0 \sim N_c - 1\}$ by N_c-point inverse fast Fourier transform (IFFT) as

$$s_{\hat{m}}(n; n_t, q) = \frac{1}{\sqrt{N_c}} \sum_{k=0}^{N_c-1} S_{\hat{m}}(k; n_t, q) \exp(i2\pi \frac{kn}{N_c}) \tag{6}$$

Finally, the last N_g samples of transmit block are copied as a cyclic prefix (CP) and inserted into the guard interval (GI), then a CP-inserted signal block of $N_g + N_c$ samples is transmitted from each transmit antenna.

B. SLM algorithm

Assuming that an N_c-length time-domain transmit block is represented by $\{s(n); n = 0 \sim N_c - 1\}$, PAPR is calculated over a V-times oversampled block, which is

$$\text{PAPR}(\{s(n)\}) = \frac{\max\{|s(n)|^2, n = 0, \frac{1}{V}, \frac{2}{V}, \ldots, N_c - 1\}}{\frac{1}{N_c} \sum_{n=0}^{N_c-1} |s(n)|^2}. \tag{7}$$

Transmit waveform of STBC-TD with Tx-FDE is different from that of STBC-TD with Rx-FDE since $S_{\hat{m}}(k; n_t, q)$ is generated based on matrix multiplication, resulting in the frequency-domain output block at each transmit antenna becomes different from $\pm D_{j,\hat{m}}(k)$ and $\pm D^*_{j,\hat{m}}(k)$. In order to keep blind data detection simple, the phase rotation in STBC-TD with Tx-FDE should follows these restrictions.

- Phase rotation should be done prior to STBC encoding. This can avoid the large number of candidates in phase rotation estimation at the receiver since it does not need to consider all combination of transmit/receive signals and phase rotation sequences at each receive antenna.
- Same phase rotation sequence should be applied to $\{d_j(n)\}$ in order to preserve the STBC code orthogonality. In addition, the phase rotation sequences can be different for different J blocks.

A set of M different unit-magnitude polyphase rotation sequences $\{p_m(n); n = 0 \sim N_c - 1, m = 0 \sim M - 1\}$ is generated in random approach as $p_m(n) \in \{e^{(i0)}, e^{(i2\pi/3)}, e^{(i4\pi/3)}\}$, except the first sequence is defined as $\{p_0(n) = e^{(i0)}; n = 0 \sim N_c - 1\}$ [6,9]. The selected phase rotation sequence $\{p_{\hat{m}}(n)\}$ is selected so as to minimize the maximum PAPR of transmit waveforms among N_t transmit antennas and Q blocks (i.e., minimax criterion), that is

$$\hat{m} = \arg \min_{m=0 \sim M-1} \left(\max_{\substack{n_t=0 \sim N_t-1, \\ q=0 \sim Q-1}} \text{PAPR}\left(\{s_m(n; n_t, q)\}\right) \right), \tag{8}$$

where $\{s_m(n;n_t,q); n = 0 \sim N_c-1\}$ is the the q-th time-domain transmit block at the n_t-th transmit antenna corresponding to the m-th phase rotation sequence. It is seen from (8) that the common phase rotation sequence is used for all $N_t \times Q$ transmit waveforms, indicating that the degree of freedom in waveform candidates generation decreases when N_t and/or N_r increase. In addition, we can alternatively select a phase rotation sequence from available B sequences for each block, but we have confirmed by computer simulation that it achieves the same PAPR performance as selecting a common sequence for all J blocks from available $M = B^J$ sequences.

III. Receiver with Phase Rotation Estimation

The receiver of STBC-TD with Tx-FDE and blind SLM, equipped with N_r receive antennas, is illustrated by Fig. 2. The propagation channel is assumed to be a symbol-spaced L-path frequency-selective block Rayleigh fading channel. The channel impulse response between the n_t-th transmit antenna and the n_r-th receive antenna is modeled as

$$h_{n_r,n_t}(\tau) = \sum_{l=0}^{L-1} h_{n_r,n_t,l}\delta(\tau - \tau_{n_r,n_t,l}), \tag{9}$$

where $h_{n_r,n_t,l}$ and $\tau_{n_r,n_t,l}$ are complex-valued path gain and time delay of the l-th path, respectively. In this paper, $h_{n_r,n_t,l}$ is assumed to be the same for Q blocks for simplicity.

The q-th block received signal at the n_r-th antenna $\{r(n;n_r,q); n = 0 \sim N_c-1\}$ is expressed by

$$r(n;n_r,q) = \sqrt{\frac{2E_s}{T_s}} \sum_{n_t=0}^{N_t-1}\sum_{l=0}^{L-1} h_{n_r,n_t,l}s_{\hat{m}}(n-\tau_{n_r,n_t,l};n_t,q)+z(n;n_r,q), \tag{10}$$

where $z(n;n_r,q)$ is an additive white Gaussian noise (AWGN) having zero mean and the variance of $2N_0/T_s$ with T_s is symbol duration. After CP removal, $\{r(n;n_r,q)\}$ is transformed into frequency domain by N_c-point FFT. The frequency-domain received signal at the k-th subcarrier can be written as an $N_r \times Q$ matrix, $\mathbf{R}(k)$, which is given by

$$\mathbf{R}(k) = \sqrt{\frac{2E_s}{T_s}}\mathbf{H}(k)\mathbf{S}_{\hat{m}}(k) + \mathbf{Z}(k), \tag{11}$$

where $\mathbf{Z}(k)$ is the frequency-domain noise matrix.

STBC decoding is carried out to obtain the spatial diversity gain. The frequency-domain decoded block $\{\hat{X}_j(k); k = 0 \sim N_c-1, j = 0 \sim J-1\}$ is determined by the following STBC decoders [10], which employ only addition/subtraction and complex-conjugate operations:

$$\hat{X}_0(k) = R(k;0,0) \qquad \text{if } N_r = 1, \tag{12a}$$

$$\begin{bmatrix} \hat{X}_0(k) \\ \hat{X}_1(k) \end{bmatrix} = \begin{bmatrix} R(k;0,0) + R^*(k;1,1) \\ R(k;0,1) - R^*(k;1,0) \end{bmatrix} \text{ if } N_r = 2. \tag{12b}$$

After STBC decoding, the received blocks before de-mapping $\{\hat{x}_j(n); n = 0 \sim N_c-1, j = 0 \sim J-1\}$ is obtained based on different transmission techniques. In SC transmission, $\{\hat{x}_j(n)\}$ is obtained by applying N_c-point inverse DFT (IDFT) to $\{\hat{X}_j(k)\}$, that is

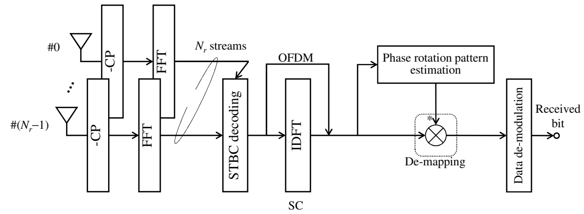

Fig. 2. Receiver with phase rotation estimation.

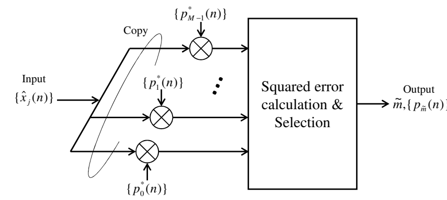

Fig. 3. Phase rotation sequence estimation algorithm.

$$\hat{x}_j(n) = \begin{cases} \frac{1}{\sqrt{N_c}}\sum_{k=0}^{N_c-1}\hat{X}_j(k)\exp(i2\pi\frac{kn}{N_c}) & \text{for SC,} \\ \hat{X}_j(n) & \text{for OFDM.} \end{cases} \tag{13}$$

In general, the received symbol blocks before data demodulation $\{\hat{d}_j(n); n = 0 \sim N_c-1, j = 0 \sim J-1\}$ is obtained by employing de-mapping, i.e. $\hat{d}_j(n) = p^*_{\hat{m}}(n)\hat{x}_j(n)$, but it requires side-information transmission. To conduct signal detection without side-information, the receiver employs phase rotation sequence estimation. The phase rotation sequence estimation exploits a fact that correct de-mapping gives very low squared error from the original constellation [7]. The estimated phase rotation sequence index $\tilde{m}$ is determined based on the following equation.

$$\tilde{m} = \arg\min_{\substack{m=0\sim M-1,\\ c\in\Psi_{\text{mod}}}} \left(\epsilon = \sum_{j=0}^{J-1}\sum_{n=0}^{N_c-1}\left|p^*_m(n)\hat{x}_j(n) - c\right|^2\right), \tag{14}$$

where Ψ_{mod} is the original data-modulated constellation. The estimation in (14) can be conducted by using ML estimation (i.e. exhaustive search) [6] or 2-step estimation using Viterbi algorithm [7], where the latter one requires much less computational complexity. The ML phase rotation sequence estimation part is depicted in Fig. 3. Finally, the received symbols for data de-modulation at the j-th block, $\{\hat{d}_j(n)\}$, is given by

$$\hat{d}_j(n) = p^*_{\tilde{m}}(n)\hat{x}_j(n). \tag{15}$$

IV. Performance Evaluation

Numerical and simulation parameters are summarized in Table I. Channel coding is not considered for simplicity. In case of transmission with side-information sharing, the minimum required side-information bits are $J\log_2 M$ [6] (which typically needs to be coded for achieving error-free transmission). Performance evaluation is done and discussed in terms of PAPR and BER.

TABLE I
SIMULATION PARAMETERS.

Transmitter	Modulation	16QAM
	No. of subcarriers	N_c = 64
	CP length	N_g = 16
	No. of transmit antennas	N_t = 1∼4
	Tx-FDE type	MMSE
SLM	Phase rotation type	Random polyphase $\{e^{(i0)}, e^{(i2\pi/3)}, e^{(i4\pi/3)}\}$
	No. of sequences	M=1∼256
Channel	Fading type	Frequency-selective block Rayleigh
	Power delay profile	symbol-spaced 16-path uniform
Receiver	No. of receive antennas	N_r=2
	Channel estimation	Ideal
	Phase rotation sequence estimation method	ML estimation

A. PAPR

PAPR performance is evaluated by measuring the PAPR value at complementary cumulative distribution function (CCDF) equals 10^{-3}, called PAPR$_{0.1\%}$. Figs. 4(a) and 4(b) show the PAPR$_{0.1\%}$ versus the number M of phase rotation sequences for OFDM and SC transmissions, respectively, both with STBC-TD and Tx-FDE. In the figures, PAPR$_{0.1\%}$ of OFDM waveform with no SLM (equals 10.6 dB) and that of SC waveform with no SLM (equals 8.4 dB) are indicated for comparison. Note that the PAPR of STBC-TD with Rx-FDE remains the same even though N_t increases [9].

The PAPR performance of OFDM transmission is firstly discussed. It is seen from Fig. 4(a) that SLM can lower the PAPR when M is large, but the PAPR reduction capability degrades when N_t and/or N_r increases. This is because the minimax criterion reduces the degree of freedom in waveform candidate generation, and hence cannot guarantee the optimal solution at each transmit antenna. Assuming M=256, the PAPR can be reduced by 3.7 dB and 3.2 dB in OFDM-STBC-TD transmission with Tx-FDE when (N_t,N_r)=(2,2) and (4,2), respectively. In addition, it is observed that the PAPR of OFDM transmission using Tx-FDE remains close to that of without Tx-FDE (about 0.1 dB difference when (N_t,N_r)=(1,1)). A possible reason is that Tx-FDE weight multiplication does not cause major changes on the correlation among OFDM subcarriers compared to one without Tx-FDE.

Meanwhile, in Fig. 4(b), the use of Tx-FDE increases PAPR by 1.6 dB when (N_t,N_r)=(1,1) in SC transmission, although it is still 0.7 dB lower than that of OFDM. A supporting reason of an increasing in PAPR when Tx-FDE is used was already described in [11] that Tx-FDE weight multiplication leads to pre-distortion in the frequency spectrum of SC signal, making the transmit spectrum become close to that of OFDM signal. However, the simulation results confirm that SLM can effectively reduce the PAPR of SC-STBC-TD with Tx-FDE. SLM can lower the PAPR by 3.3 dB and 2.8 dB in SC-STBC-TD with Tx-FDE when (N_t,N_r)=(2,2) and (4,2), respectively, and assuming M=256. It is also seen that PAPR increases when N_t increases due to the disadvantage of minimax criterion, which is similar to the case of OFDM-STBC-TD.

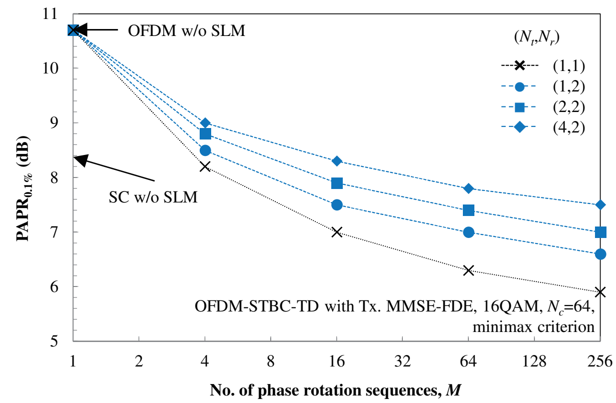

(a) OFDM transmission

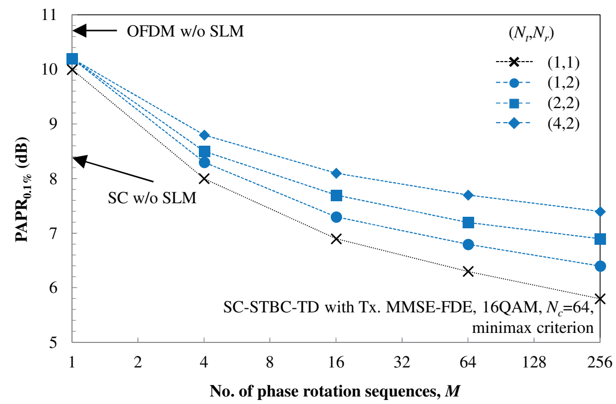

(b) SC transmission

Fig. 4. PAPR$_{0.1\%}$ versus the number of candidates.

It is worthwhile to notice from Fig. 4 that the difference of PAPR between OFDM-STBC-TD using Tx-FDE and SC-STBC-TD using Tx-FDE is very small when N_t and M are large, i.e., only 0.1 dB difference when (N_t,N_r)=(4,2) and M=256. This indicates that there is no significant advantage in aspects of PAPR between OFDM and SC when Tx-FDE and SLM are used.

B. BER performance

Fig. 5 shows the uncoded BER performances of STBC-TD with Tx-FDE and blind SLM as a function of total received $E_b/N_0 = (1/N_{\text{mod}})(E_s/N_0)(1 + N_g/N_c)$ with N_{mod} being modulation level (4 for 16QAM). Performances of OFDM transmission and SC transmission are plotted in Figs. 5(a) and 5(b), respectively. The number of transmit and receive antennas for STBC-TD (N_t,N_r) is assumed to be (1,1), (2,2) and (4,2). BER of STBC-TD with Tx-FDE and SLM with side-information transmission is also provided for comparison, where the side-information detection is assumed to be ideal. The number of phase rotation sequences is set to be M=64.

It is seen from Fig. 5 that BER improves when either N_t or N_r increases due to an increasing of spatial diversity gain. The BER of SC-STBC-TD (shown in Fig. 5(b)) is better than that of OFDM-STBC-TD in every (N_t,N_r) case. This is because the combination of SC transmission and MMSE-

FDE can obtain the frequency diversity gain [12] regardless of whether the FDE is applied at the transmitter or the receiver. The BER performances of transmissions using blind SLM degrades compared to those of SLM with ideal side-information detection when the transmit power is low. This is consistent with [6,9] since the noise power makes the received symbols become apart from the original constellation even when the de-mapping is done correctly. However, it is seen that there is no difference on BER of blind SLM and SLM with side-information, both OFDM-STBC-TD and SC-STBC-TD, when the received E_b/N_0 is higher than about 5 dB.

In summary, although the results in Sect.IV-A indicate that there is no significant difference in aspect of PAPR between OFDM-STBC-TD and SC-STBC-TD with Tx-FDE and blind SLM. The simulation results shown by Fig. 5 also indicate that SC-STBC-TD can be considered as a better option than OFDM-STBC-TD in terms of uncoded BER performance. However, the BER performance of STBC-TD with Tx-FDE, blind SLM, and forward error-correction coding (FEC) has not been yet considered. Therefore, the performance evaluation considering FEC is left as our important future work.

V. Conclusion

Blind SLM technique for STBC-TD with Tx-FDE was introduced in this paper. The SLM employs a selected common phase rotation pattern for all N_t transmit antennas, where the phase rotation pattern is obtained based on the minimax criterion. An arbitrary number N_t of transmit antennas can be used without reducing STBC code rate. Computer simulation results confirmed that the blind SLM can lower the PAPR of both OFDM and SC signals by 2.8-3.7 dB when M=256 and N_t=2 or 4. It was also shown that no significant BER degradation occurs at high-E_b/N_0 region (i.e. higher than 5 dB) even though no side-information transmission is required.

In addition, there still exist rooms for improvement on blind SLM, especially in aspects of estimation accuracy and computational complexity in the phase rotation sequence estimation. An appropriate design on codebook and phase rotation sequences may be considered as a key in our future study to further improve the blind SLM.

Acknowledgment

This paper includes a part of results of "The research and development project for realization of the fifth-generation mobile communications system" commissioned to Tohoku University by The Ministry of Internal Affairs and Communications (MIC), Japan.

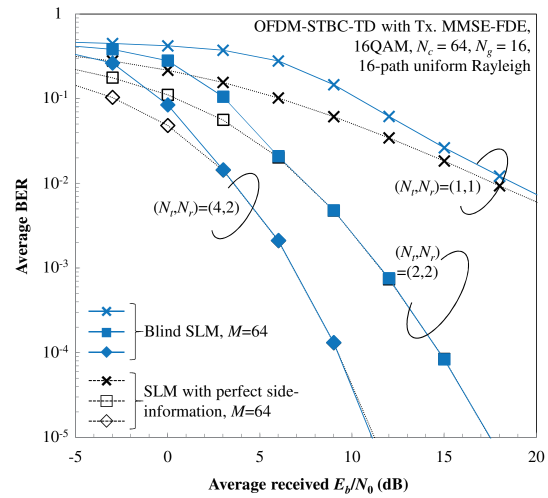

(a) OFDM transmission

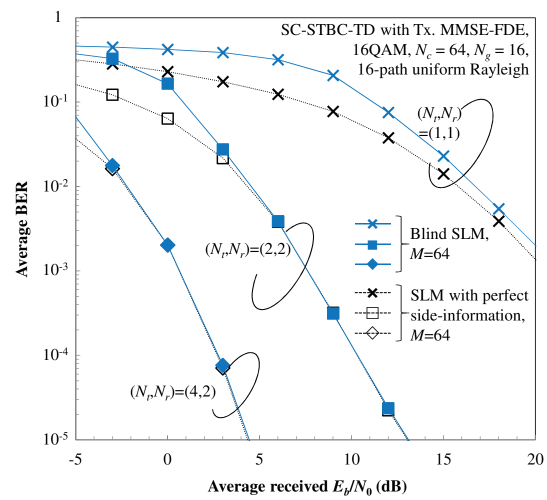

(b) SC transmission

Fig. 5. Uncoded BER performance.

References

[1] DOCOMO 5G White Paper, 5G Radio Access: Requirements, Concept and Technologies, Jul. 2014.

[2] W. L. Chan and J. R. Long, "A 58-65 GHz Neutralized CMOS Power Amplifier with PAE above 10% at 1-V Supply," *IEEE Journal of Solid-State Circuits*, Vol. 45, No. 3, pp. 554-564, Mar. 2010.

[3] H. G. Myung et al., "Single Carrier FDMA for Uplink Wireless Transmission," *IEEE Veh. Technol. Mag.*, Vol. 1, No. 3, pp. 30-38, Sept. 2006.

[4] H. Ochiai, "On Instantaneous Power Distributions of Single-Carrier FDMA Signals," *IEEE Wireless Commun. Lett.*, Vol. 1, No. 2, pp. 73-76, Jan. 2012.

[5] R. W. Bauml et al., "Reducing the Peak-to-Average Power Ratio of Multicarrier Modulation by Selected Mapping," *IEEE Electron. Lett.*, Vol. 32, No. 22, pp. 2056-2057, Oct. 1996.

[6] A. Boonkajay and F. Adach, "A Blind Polyphase Time-Domain Selected Mapping for Filtered Single-Carrier Signal Transmission," *Proc. IEEE Veh. Technol. Conference (VTC 2016-Fall)*, Montreal, Canada, Sept. 2016.

[7] A. Boonkajay and F. Adachi, "2-Step Signal Detection for Blind Time-Domain Selected Mapping," *IEICE Tech. Rep.*, Vol. 116, No. 257, RCS2016-182, pp. 161-166, Oct. 2016.

[8] S. M. Alamouti, "A Simple Transmit Diversity Technique for Wireless Communications," *IEEE J. Select. Areas. Commun.*, Vol. 16, No. 8, pp. 1451-1458, Oct. 1998.

[9] A. Boonkajay and F. Adachi, "Blind Selected mapping Techniques for Space-Time Block Coded Filtered Single-Carrier Signals," *Proc. IEEE VTS Asia Pacific Wireless Commun. Symp. (APWCS2016)*, Tokyo, Japan, Aug. 2016.

[10] H. Tomeba et al., "Frequency-domain Space-Time Block Coded-Joint Transmit/Receive Diversity for Direct-Sequence Spread Spectrum Signal Transmission," *IEICE Trans. Commun.*, Vol. E90-B, No. 3, pp. 597-606, Mar. 2007.

[11] S. B. Slimane, "Reducing the Peak-to-Average Power Ratio of OFDM Signals Through Precoding," *IEEE Trans. Veh. Technol.*, Vol. 56, No. 2, pp. 686-695, Mar. 2007.

[12] F. Adachi et al., "Broadband CDMA Techniques," *IEEE Wireless Commun. Mag.*, Vol. 12, No. 2, pp. 8-18, Apr. 2005.